A series of new structural models for the OEC in photosystem II†

Ian J. Hewitt,[a] Jin-Kui Tang,[a] N. T. Madhu,[a] Rodolphe Clérac,[b] Gernot Buth,[c] Christopher E. Anson[a] and Annie K. Powell*[a]

Received (in Cambridge, UK) 12th December 2005, Accepted 13th February 2006
First published as an Advance Article on the web 2nd March 2006
DOI: 10.1039/b518026k

A new series of MMn^{II-III}_4 clusters (M = Na, Ca) has been structurally characterised and their relevance to understanding the oxygen evolving centre of photosystem II is discussed.

The oxygen evolving centre (OEC) of photosystem II (PSII) is part of the complex biological machinery enabling photosynthesis in green plants and cyanobacteria. There is good evidence from protein crystallography, EXAFS and EPR studies that the active core is composed of an aggregation of up to five metal centres that have been identified as one Ca^{2+} and four Mn centres.[1] Kok proposed that the water splitting process is achieved by cycling the Mn centres through different oxidation levels to give five states designated S_i (i = 0, 1, 2, 3 or 4).[2] It has also been shown that Cl^- and Ca^{2+} ions are required to proceed past the S_3 state.[3,4]

Much effort has been expended in producing possible models for the OEC, initially when very little was known about the composition of the centre in terms of nuclearity and connectivity and, indeed, before the importance of the Ca^{2+} and Cl^- cofactors had been realised. The models have been primarily proposed to help in the identification of the structural features in the native system using methods such as EXAFS, EPR and electronic absorption spectra in conjunction with high resolution X-ray crystal structure analysis of the small molecule analogues. The four recent protein X-ray crystallographic studies[5–8] at resolutions from 3.2 and 3.8 Å present various models for the cluster of metal centres at the heart of PSII, but there are serious discrepancies amongst these and although the favoured interpretation assigns the core to a Mn_4CaO_4 cluster assembly with a cubane motif,[7] a recent X-ray absorption study has suggested that the details of this could be in serious doubt due to X-ray induced damage.[9] In order to split water the OEC must transfer a total of four electrons which is thought to be achieved through changing the oxidation levels of the Mn centres in the various S states. However, a survey of the literature reveals that the actual oxidation levels of the Mn centres in these states is still a matter of some considerable debate. For example, in discussing the mechanism of oxygen evolution Brudvig and Crabtree acknowledge that three possibilities consistent with EPR data exist for all of the S levels.[10] Thus, for example, S_0 could correspond to $Mn^{II}_3Mn^{III}$, $Mn^{II}Mn^{III}_3$ or $Mn^{III}_3Mn^{IV}$. On the basis of XAS data many other workers tend to favour S states with the higher oxidation levels, but the possibility that the interaction with X-rays in the experiments might lead to artificially high oxidation states cannot be excluded. On the other hand, one of the "textbook versions" of events is firmly on the side of the lower oxidation levels.[11] There thus seems to be an urgent need for new model compound systems with core structures which could help to resolve these difficulties.

We have been able to synthesise and structurally characterise three pentanuclear metal aggregates, **1–3**, which provide promising candidates:

$$[CaMn^{III}_3Mn^{II}(\mu_4\text{-}O)L_3Cl_2(O_2CMe)_{1.2}(H_2O)_{1.5}\text{-}(MeOH)_{0.3}]Cl_{0.8}\cdot 5MeOH \quad (1)$$

$$[NaMn^{III}_3Mn^{II}(\mu_3\text{-}O)L_3(N_3)_{2.7}(O_2CMe)_{1.3}(MeOH)]\cdot 2MeOH\cdot 0.5H_2O \quad (2)$$

$$[\{NaMn^{III}_4(\mu_3\text{-}O)L'_4(N_3)_3(MeOH)\}_2]Cl\cdot 3MeOH \quad (3)$$

These complexes are readily obtained by the reaction of divalent manganese salts with the Schiff-base ligands L and L′ (Fig. 1) which are formed by the *in-situ* condensation of *o*-vanillin with 2-hydroxypropylamine or 2-aminopropan-1,3-diol, respectively, and in the presence of triethylamine and either $CaCl_2$ or NaN_3.†‡ Such Schiff-base ligands are useful for stabilising manganese in the +III oxidations state, as has been noted in other studies on modelling aspects of PSII.[12]

The central core of the structures of compounds **1** and **2** consists of three Mn^{III} centres (Mn(1)–Mn(3)), each of which is chelated by a tridentate ligand L *via* the deprotonated phenol and propanol oxygens and the imino nitrogen (Fig. 2). These are linked through an oxo ligand O(1), such that the mean planes of the ligands are approximately perpendicular to the planar Mn_3O moiety. Two monodentate ligands, (μ-Cl) in **1** or (μ,η^1-N_3) in **2**, and a bidentate acetate provide further bridges between these three Mn^{III} centres to give an isosceles Mn_3O triangle with two shorter Mn···Mn distances and one longer.

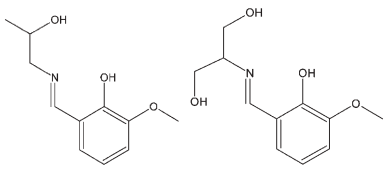

Fig. 1 The Schiff-base ligands L (condensed from *o*-vanillin and 2-hydroxypropylamine, left) and L′ (from *o*-vanillin and 2-aminopropan-1,3-diol, right).

[a]*Institut für Anorganische Chemie, Universität Karlsruhe, Engesserstrasse 15, Geb. 30.45, D-76128, Karlsruhe, Germany. E-mail: powell@chemie.uni-karlsruhe.de; Fax: (+49) 721 608 8142; Tel: (+49) 721 608 2135*
[b]*Centre de Recherche Paul Pascal, CNRS UPR 8641, 115 Avenue du Dr. A. Schweitzer, 33600, Pessac, France*
[c]*Institut für Synchrotronstrahlung, Forschungszentrum Karlsruhe, D-76344, Eggenstein-Leopoldshafen, Germany*
† Electronic supplementary information (ESI) available: Bond Valence Sum calculations and synthetic procedures. See DOI: 10.1039/b518026k

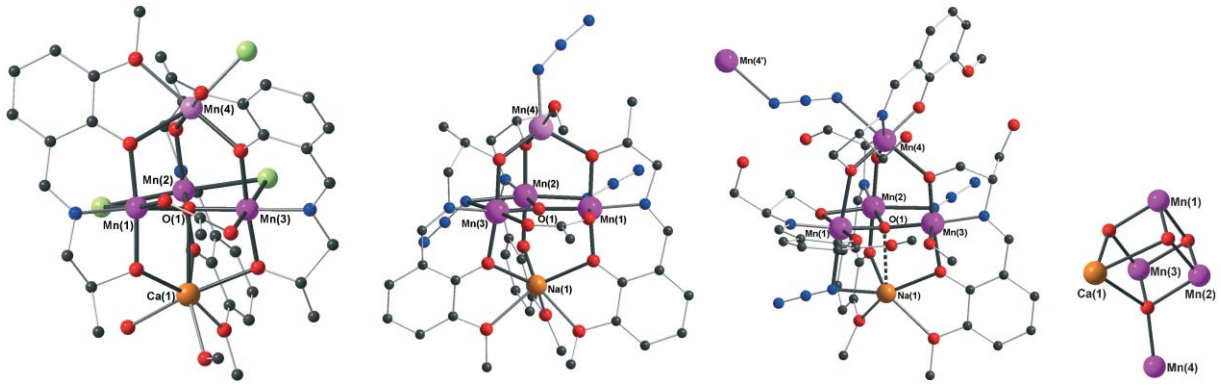

Fig. 2 Structures of (left to right): Compounds **1**, **2**, **3** and the proposed metal core arrangement of the OEC from the protein structure of *Thermosynechococcus elongatus*.[7] (For clarity, in **1** and **3**, minor disorder components have been omitted.) Mn^{III} purple, Mn^{II} pink, Na or Ca orange, O red, C black, N blue, Cl pale green.

In **1**, one of the three ligands L is oriented antiparallel to the other two. Two deprotonated phenol and one deprotonated propanol oxygens bridge to Mn(4) with a terminal chloride completing the coordination sphere. Conversely, two deprotonated propanol and one deprotonated phenol oxygens bridge to the Ca^{2+} cation Ca(1), which is further ligated by the central oxo ligand, a water and a disordered mixed monodentate ligand.

In **2**, the three ligands are oriented mutually parallel. The three deprotonated propanol oxygens each bridge between their respective Mn^{III} and the Mn^{II} centre, Mn(4), while on the other side of the Mn_3O triangle the three deprotonated phenol oxygens each bridge to Na(1) with the three methoxy groups providing additional chelation of the Na^+ cation. The coordination sphere of Mn(4) is completed by a methanol ligand and a disordered mixed anion (70% N_3/30% acetate).

In compound **3**, Mn(1)–Mn(4) are all Mn^{III} and the structural pattern found in **1** and **2** has been modified, in particular by the presence of four ligands L′. Two ligands adopt the same structural motif as in **2**, with their alkoxo oxygens bridging to the apical Mn(III), Mn(4), and the deprotonated phenol and methoxy oxygens ligating Na(1). However, the ligand that chelates the third central Mn is now rotated so that it lies close to coplanar with the Mn_3O triangle and the alkoxo oxygen forms a monodentate bridge across one edge of the triangle. An end-on azide ligand bridges the second short edge of the Mn_3O unit, while the long edge is now occupied by a hydrogen bond from a methanol ligand to the deprotonated phenol oxygen of the parallel ligand. The fourth ligand chelates the apical Mn(4) with its alkoxo oxygen forming the remaining bridge to the Mn_3O triangle. A (1,3-η^1,η^1-N_3) ligand bridges between Mn(4) and Mn(4′) of an inversion-related cluster, forming a weak dimer. For all three compounds the oxidation states assigned to the Mn centres were checked using Bond Valence Sum calculations (see supplementary data†).[13]

The interpretation of the structure of the core which is currently postulated[7] has an arrangement of the metals which can be regarded as defining a trigonal bipyramid and the relation between this and our compounds is depicted in Fig. 3. In our compounds the equatorial site M_1, which is thought to be occupied by the Ca^{2+} in the protein structure, corresponds to a Mn centre whereas the apical M_2 site, which is thought to be an Mn centre in the protein structure, corresponds to a Ca or Na centre in our compounds.

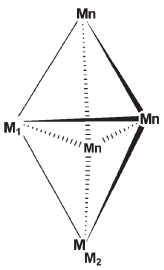

Compound	M_1	M_2
1	Mn	Ca
2, **3**	Mn	Na
OEC	Ca	Mn

Fig. 3 Schematic diagram of the $Mn_3M_1M_2$ core in compounds **1**, **2** and **3** and in the OEC in PSII.

Within the equatorial plane of the OEC core there is only one Mn···Mn distance and at 2.7 Å this is significantly shorter than observed in compounds **1–3** (see Table 1) where the shortest distance observed is 3.0 Å for neighbouring Mn^{III} ions in **3**. Likewise, comparing the distances between apical and equatorial sites in the OEC, Mn1 is on average closer to the equatorial plane than Mn4 with Mn1···M_{eq} = 2.7–3.3 Å; Mn4···M_{eq} = 3.2–4.0 Å. In the model compounds **1–3**, however, the apical sites are at similar distances with M_{ap}···M_{eq} = 3.4–3.7 Å. It must be noted, however, that neither the Mn oxidation states nor the Kok state in the protein crystal structure have been unequivocally determined. It seems likely from the data from the protein structure with the rather short Mn···Mn distances that the oxidation states of the Mn centres are higher than the ones we assign in the model compounds.

Table 1 Comparison of M···M distances in **1–3** with those in the Mn_4Ca cluster in the OEC of *Thermosynechococcus elongatus*[7]

	1	**2**	**3**		**OEC**
Mn1–Mn2	3.275	3.171	3.015	Mn2–Mn3	2.722
Mn2–Mn3	3.225	3.152	3.100	Mn2–Ca1	3.393
Mn1–Mn3	3.398	3.452	3.534	Mn3–Ca1	3.371
Mn1–Mn4	3.512	3.402	3.730	Mn4–Mn2	3.245
Mn2–Mn4	3.437	3.435	3.512	Mn4–Mn3	3.225
Mn3–Mn4	3.531	3.453	3.646	Mn4–Ca1	3.950
M1–Mn1	3.437	3.475	3.497	Mn1–Mn2	2.658
M1–Mn2	3.452	3.470	3.379	Mn1–Mn3	2.678
M1–Mn3	3.358	3.451	3.383	Mn1–Ca1	3.344
M1–Mn4	5.763	5.772	5.981	Mn1–Mn4	5.125
M1 =	Ca1	Na1	Na1	Mn1	

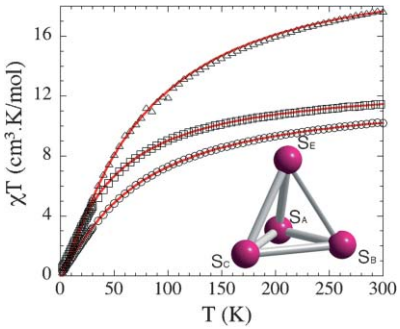

Fig. 4 Plot of the χT product vs. T (where χ is M/H) measured at 1000 Oe for **1** (○), **2** (□) and **3** (△). Red solid lines are the best fits obtained with the model described in the text. Inset: Scheme of the spin topology in compound **1–3**.

Comparing the magnetic properties of these models with the reported results on the OEC in various S states is further complicated by the lack of agreement on the oxidation levels on the Mn centres in the various states. However Messinger *et al.* have reported the detection of an EPR multi-line signal at X-band from a known S_0 state which can be understood as arising from an S = ½ ground state.[14]

We investigated the magnetic properties of compounds (**1–3**) between 1.8 and 300 K using a Quantum Design SQUID magnetometer MPMS-XL. On lowering the temperature all the compounds exhibit a decrease of their χT product indicating the presence of dominating antiferromagnetic interaction between Mn spins (Fig. 4). On the basis of their molecular structures we have tried to simulate the susceptibility in the frame of an isotropic Heisenberg model. Given the number of magnetic centres and the presence of 6 non-equivalent couplings, similar bridges linking Mn ions were considered identical in the fitting and bridging modes mediating magnetic interactions known to be weak were ignored in order to avoid over-parameterization. The final Hamiltonian used for **1** and **2** was: $H = -2\,J_1\,(S_E\cdot(S_A + S_B + S_C)) - 2\,J_2\,(S_A\cdot S_C) - 2\,J_3\,(S_B\cdot(S_A + S_C))$ and for **3**: $H = -2\,J_1\,(S_E\cdot S_C) - 2\,J_3\,(S_A\cdot S_B)$. In this way we were able to simulate all the experimental data with the parameters displayed in Table 2. This analysis leads to the conclusion that compounds **1**, **2** and **3** possess $S_T = 1/2$, $S_T = 1/2$ and $S_T = 0$ ground states respectively. These data together with oxidation levels for the Mn centres suggest that compounds **1** and **2** serve as possible models for the metal core in the OEC with an S_0 Kok state in the $Mn^{II}Mn^{III}{}_3$ version and compound **3** to the S_1 state in the $Mn^{III}{}_4$ representation.

In summary, these compounds will be of assistance in understanding more about the OEC by providing well-defined models with plastic coordination geometries. As can be seen by comparing the formulae of compounds **1–3**, it is possible to interchange metal centres in the core as well as the auxiliary ligands such as chloride and azide. An obvious first goal is to synthesise a compound with a Ca in the equatorial plane of the trigonal bipyramid and higher oxidation level compounds are also a priority. We will also use the models to compare and calibrate EXAFS data including gauging the possible effects of radiation damage and we also plan other spectroscopic studies such as UV/Vis and EPR. This will allow for a systematic exploration of features which have been identified as being important in shedding light on the structures and electronic properties of the various Kok states in the OEC.

Table 2 Magnetic parameters for compounds **1–3**

	1	**2**	**3**
S_A, S_B, S_C, S_E	2, 2, 2, 5/2	2, 2, 2, 5/2	2, 2, 2, 2
J_{AB}/k_B	J_3/k_B = 0(1) K	J_3/k_B = 0.0(8) K	J_3/k_B = −6.0(5) K
J_{BC}/k_B	J_3/k_B = 0(1) K	J_3/k_B = 0.0(8) K	fixed at 0 K
J_{CA}/k_B	J_2/k_B = −10.0(5) K	J_2/k_B = −8.0(5) K	fixed at 0 K
J_{EA}/k_B	J_1/k_B = −5.0(5) K	J_1/k_B = −3.0(5) K	fixed at 0 K
J_{EB}/k_B	J_1/k_B = −5.0(5) K	J_1/k_B = −3.0(5) K	fixed at 0 K
J_{EC}/k_B	J_1/k_B = −5.0(5) K	J_1/k_B = −3.0(5) K	J_1/k_B = −18.0(5) K
g	1.94(1)	1.97(1)	1.87(1)

This work was supported by the CNRS, the University of Bordeaux I; the Conseil Regional d'Aquitaine; the D.F.G. SPP 1137 and Center for Functional Nanostructures, and QuEMolNa MRTN-CT 2003-504880.

Notes and references

‡ **1**: A very small crystal (0.08 × 0.012 × 0.005 mm) of **1** was measured to 0.88 Å resolution on the ANKA-SCD synchrotron beamline at the Forschungszentrum Karlsruhe using λ = 0.7999(2) Å radiation. $C_{40.7}H_{66.8}CaCl_{3.8}Mn_4N_3O_{19.2}$ (1299.20 g mol^{-1}); triclinic, a = 12.7590(12), b = 14.3574(14), c = 15.6647(17) Å, α = 88.148(9), β = 83.900(8), γ = 82.349(8)°, U = 2827.4(5) Å^3, T = 150 K, $P\bar{1}$, Z = 2, μ(Mo–K$_\alpha$) = 1.399 mm^{-1}, F(000) = 1340; 15575 data measured, 7959 unique (R_{int} = 0.1136), final wR_2 (F^2, all data) = 0.2277, S = 1.076, R_1 (5019 with $I > 2\sigma(I)$) = 0.0849. **2**: $C_{38.6}H_{55.9}Mn_4N_{11.1}NaO_{16.1}$ (1175.79 g mol^{-1}); rhombohedral, a = 50.422(4), c = 10.6912(8) Å, U = 23540(5) Å^3, T = 100 K, $R\bar{3}$, Z = 18, μ(Mo–K$_\alpha$) = 1.026 mm^{-1}, F(000) = 10890; 30242 data measured, 10197 unique (R_{int} = 0.0930), final wR_2 (F^2, all data) = 0.0923, S = 0.989, R_1 (4635 with $I > 2\sigma(I)$) = 0.0505. **3**: $C_{93}H_{132}ClMn_8N_{23}Na_2O_{39}$ (2717.17 g mol^{-1}); triclinic, a = 13.7526(6), b = 14.1250(7), c = 15.6463(7) Å, α = 90.093(1), β = 94.081(1), γ = 110.112(1)°, U = 2845.5(2) Å^3, T = 100 K, $P\bar{1}$, Z = 1, μ(Mo–K$_\alpha$) = 0.982 mm^{-1}, F(000) = 1402; 12204 data measured, 10325 unique (R_{int} = 0.0711), final wR_2 (F^2, all data) = 0.02138, S = 0.994, R_1 (6826 with $I > 2\sigma(I)$) = 0.0695. CCDC numbers 293107–293109. For crystallographic data in CIF or other electronic format see DOI: 10.1039/b518026k

1 For a recent review see: S. Mukhopadhyay, S. K. Mandal, S. Bhaduri and W. H. Armstrong, *Chem. Rev.*, 2004, **104**, 3981–4026.
2 B. Kok, B. Forbush and M. McGloin, *Photochem. Photobiol.*, 1970, **11**, 457.
3 C. Critchley, *Biochem. Biophys. Acta*, 1985, **811**, 33; W. J. Coleman, *Photosynth. Res.*, 1990, **23**, 1.
4 A. Boussac, B. Maison-Peteri, A.-L. Etienne and C. Vernotte, *Biochim. Biophys. Acta*, 1985, **808**, 231; A. Boussac and A. W. Rutherford, *Chem. Scr.*, 1988, **28A**, 123.
5 A. Zouni, H.-T. Witt, J. Kern, P. Fromme, N. Krauss, W. Saenger and P. Orth, *Nature*, 2001, **409**, 739.
6 N. Kamiya and J. R. Shen, *Proc. Natl. Acad. Sci. U. S. A.*, 2003, **100**, 98.
7 K. N. Ferreira, T. M. Iverson, K. Maghlaoui, J. Barber and S. Iwata, *Science*, 2004, **303**, 1831.
8 J. Biesiadka, B. Loll, J. Kern, K.-D. Irrgang and A. Zouni, *Phys. Chem. Chem. Phys.*, 2004, **6**, 4733.
9 J. Yano, J. Kern, K.-D. Irrgang, M. J. Latimer, U. Bergmann, P. Glatzel, Y. Pushkar, J. Biesiadka, B. Loll, K. Sauer, J. Messinger, A. Zouni and V. K. Yachandra, *Proc. Natl. Acad. Sci. U. S. A.*, 2005, **102**, 12047.
10 G. W. Brudvig and R. H. Crabtree, *Proc. Natl. Acad. Sci. U. S. A.*, 1986, **83**, 4586.
11 *The Biological Chemistry of the Elements*, J. J. R. Fraústo da Silva and R. J. P. Williams, Oxford University Press, Oxford, 1994.
12 C. Hureau, E. Anxolabéhère-Mallart, G. Blondin, E. Rivière and M. Nierlich, *Eur. J. Inorg. Chem.*, 2005, 4808.
13 W. Liu and H. H. Thorp, *Inorg. Chem.*, 1993, **32**, 4102; N. E. Brese and M. O'Keefe, *Acta Crystallogr., Sect. B: Struct. Sci.*, 1991, **B47**, 192.
14 J. Messinger, J. H. Robblee, W. On Yu, K. Sauer, V. K. Yachandra and M. P. Klein, *J. Am. Chem. Soc.*, 1997, **119**, 11349.

